FF ANALYSIS AND GNC CONCEPT FOR A FF MISSION IN HIGHLY ECCENTRIC ORBIT

E. Di Sotto[(1)], L.F. Peñín, [(2)], J.C. Bastante[(3)], A. Marcos[(4)], J. Branco [(5)]

[(1,3,,5)]DEIMOS ENGENHARIA S.A., Av. D.João II, Lt. 1.17, Edifício Torre Zen, 10º, Lisbon, Portugal
[(1)] emanuele.disotto@deimos.com.pt
[(3)] juan-carlos.bastante@deimos.com.pt
[(5)] joao.branco@deimos.com.pt

[(2,4)] DEIMOS SPACE S.L, Ronda de Poniente 19,Edificio Fiteni VI, P. 2, 2º28760 Tres Cantos,Madrid, Spain
[(2)] luis-felipe.penin@deimos-space.com
[(4)] andres.marcos@deimos-space.com

ABSTRACT

Missions requiring spacecraft flying in formation are currently being investigated in all space domains. Formation Flying (FF) technologies will provide the leap in performances required for future missions in Science, Earth (and planetary) Observation and also space application areas not yet established, e.g. advanced civil security, space exploration.
Firstly this paper addresses in details the FF analysis aiming at the characterization of a baseline mission scenario in a highly eccentric orbit, including definition of FF strategies and corresponding operational modes and GNC system properties.
Based on this characterization, a proper GNC system concept is presented especially stressing those aspects related with GNC algorithms. Relative motion peculiarities into high elliptical orbit demand for novel algorithms, especially for Guidance and Control (time-variant plant) and dynamics modelisation within the navigation filter.

1. INTRODUCTION

This work addresses the GNC design for a Formation Flying mission in highly eccentric orbit (>0.7). Before entering in the details of the GNC system design, an exhaustive analysis and definition of the reference scenario has been performed and it is reported in sec. 2.

Proba-3 has been selected as the reference mission scenario for the application GNC concept developed and proposed within this paper for FF in High Elliptical Orbit (HEO). Proba-3 is a Formation Flying (FF) Mission currently under development by ESA for the application of technologies enabling future formation flying missions (command and control architectures, sensors, actuators, GNC, etc.). As a complementary objective, Proba-3 will embark as a payload a coronagraph to observe the Sun corona. It requires 2 spacecraft, one spacecraft carries the sun occulter and the other spacecraft carries the coronagraph instrument.

This analysis allows the identification of an applicable set of mission requirements, constraints and system drivers which lead to the proper design of the GNC system. Main concepts for the GNC system design have been detailed in section 3.

GNC design relies on a navigation system based on optical and RF sensors depending on the different phases identified in the reference mission profile.
The main feature of the high eccentric orbit, considered within this study, is represented by the relative dynamics modelisation that affects all the different GNC functions.

Relative dynamics into elliptical orbit can be effectively linearised however the resulting plant is time-variant. This increases the complexity when deriving the proper closed loop controller, and makes quite challenging the design of the proper guidance algorithms and the dynamics model to be handled within the navigation filter.

Controller design has been faced using a NDI approach using as desired dynamics the one coming out from a PID controller actuating on the reference position provided through the guidance.

Relative dynamics implemented within navigation filter and guidance schemes is an analytical solution available in literature (Yamanaka-Ankersen solution [1]) that has been enhanced with the system response to a constant force in both: the local reference system (LVLH) and the inertial reference system.

This represents an important asset for an efficient on-board assessment of the forced relative dynamics when either control force is considered (within the navigation filtering process) or SRP is taken into account within direct retargeting guidance scheme (see *Figure 3-1*).

Proc. 3rd Int. Symp. on Formation Flying, Missions and Technologies, Noordwijk ,The Netherlands,
23-25 April 2008 (ESA SP-654, June 2008)

2. FF ANALYSIS AND BASELINE SCENARIO

FF analysis aims at the characterization of a baseline mission scenario including: definition of FF strategies, correspondent operational mode and GNC system.

Mission Concept

The objective of the Proba3 mission is to demonstrate FF technology and at the same time be able to provide scientific return. A High Elliptical Orbit (HEO) orbit is selected due to its quiet gravitational environment around the apogee. The former baseline used for this work was a 24 h orbit with a perigee of 800 km.

The mission concept is based on performing a Formation inertial pointing for scientific experiments (Sun observation) around the apogee passage. Part of the mission plan shall be also dedicated to conduct demonstration experiments of FF maneuvers.

The mission is de-composed into different phases as follows (Figure *2-1*):

- Experiment / demonstration phase: Scientific experiment and FF manoeuvres demonstration experiments will be done around the apogee where the environment is quieter for each orbit.

- Non-experimental phase: distributed along the part of the orbit close the perigee where conducting experiments could be excessively costly.
  The approach is to minimize the required control needs. The ideal objective is to be able to completely leave the spacecraft in open-loop being confident that there is no collision between them and that after the perigee passage it does not cost much to go back to the required configuration.

- Deployment phase: ranges from exit from the dispenser to acquiring a given configuration close the required one for either the FF demonstration or the scientific experiment. After, de-tumbling and cancelling the relative velocity of the spacecraft a formation deployment shall be performed to reach the required configuration from the initial random distribution to start the experiments.

In this context, geometry of Sun with respect to the subject formation satellites is an important problem variable. Sun direction can be expressed by two angles:

- DEC is the Sun declination with respect to the orbital plane, that is, the angle of Sun direction with the orbital plane;
- RAS is the Sun right ascension with respect to apogee line; that is, the angle formed by the Sun direction projection on the orbital plane and the line of apsides.

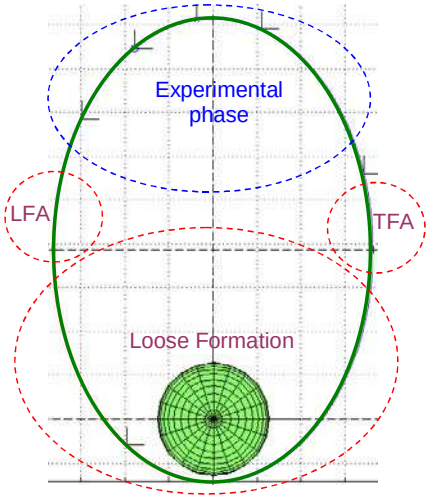

Figure 2-1 Segmentation of the orbit into experimental and non-experimental phases

Also, a classical LVLH frame shall be considered for FF relative motion description in the local orbital frame, with Z axis along Nadir, and Y axis opposite to the orbital angular moment

Inertial pointing Formation Experiment

Figure 2-2 shows the evolution of the Sun direction as projected onto the reference orbital plane during the mission life. As it was expected, low declination angles are obtained, while right ascension covers the whole possible range once per year

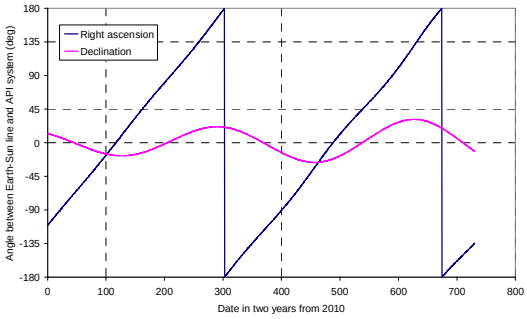

Figure 2-2 Sun evolution wrt the orbital plane

Operational scientific experiments consist in having the two-spacecraft formation axis inertially pointed to the Sun, while the inter-satellite distance is held constant and equal to 150 m.
Figure 2-3 shows the cost per experiment (i.e., per passage around apogee) as a function of time from mission start, and for the two considered experiment durations.
As it can be seen, there is a strong correlation between these plots and right ascension of Sun

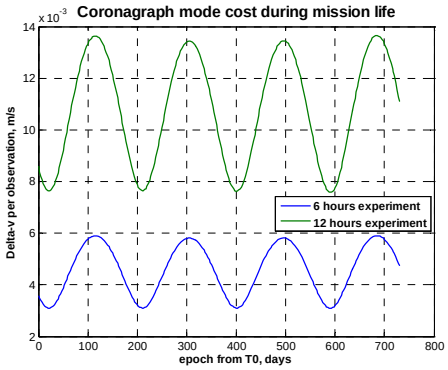

Figure 2-3 ΔV for science phase along mission timeline

The reason for this (expected) behaviour is that a radial (either outwards or inwards) displacement at apogee constitutes the less Keplerian condition at that orbital point, and as such, the cost of keeping this configuration must be higher.

Table 1 shows the cost of maintaining the formation for the experimental phase during the 2 year mission for the two experiment lengths, considering the need to compensate for differential Solar Radiation Pressure (SRP)

Experiment	Keplerian	SRP	Total
6 hours Inertial	2.88 m/s	2.49 m/s	5.37 m/s
12 hours Inertial	6.76 m/s	4.88 m/s	11.64 m/s

Table 1 Cost of scientific experiments for 2 years mission

FF Manoeuvres Experiment

The purpose of this section is to present the analyses run on FF manoeuvres demonstration to be performed within the reference scenario

The aim is to compute the required ΔV per manoeuvre, considering different orbital positions for the execution of the manoeuvre, different durations, and the complete range of relative positions between the Sun and the reference orbital plane that will be experienced during the whole mission life-time

The considered manoeuvres were specified as:

- Decentralised rotation. Starting from a science configuration (i.e., both satellites aligned with Sun direction), flyer rotates by 5º at a distance of 150 m from master considering two possible axes for rotation: normal to the reference orbital plane and normal to the line of sight between both spacecraft and contained in the plane normal to the reference orbital plane.

- Centralised rotation. Starting from a science configuration, master manoeuvres to acquire an offset wrt Sun axis, in order to start a rotation around the original flyer-Sun direction with a cone aperture angle of 4º.

- Resizing. Flyer will move along the baseline axis in accordance to a given pre-defined guidance profile. Resizing distances of 1m and 5 m will be tested.

- Coarse retargeting. A manoeuvring sequence is imposed on flyer in order to acquire a lateral displacement with respect to baseline direction of around 13m. The formation is not constrained during the manoeuvre, i.e., there is no active control to follow a pre-defined profile.

Figure 2-4 shows as an example the ΔV for a centralised rotation of 20º around baseline, cone aperture angle of 4º for duration of 1 hour, depending on the location of the manoeuvre within the orbit.

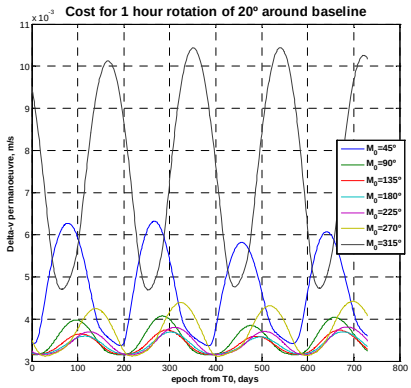

Figure 2-4 Centralised rotation of 20º around baseline, cone aperture angle of 4º. ΔV for a manoeuvre duration of 1 hour

From the analyses performed, the following conclusions were extracted:

- Effect of location in the orbit:
  - Small anomalies (< 90 deg) give relatively high values with respect other anomalies and tend to reduce with manoeuvre time (depart from perigee)
  - Large anomalies (>270 deg) give excessive high values and are aggravated with large manoeuvre times (approach perigee)
  - Anomalies within 90-270 deg provide similar values with no significant difference between them for all the manoeuvres

- Effect of Epoch: large variation with epoch of manoeuvres close to the perigee, and specifically of decentralised rotation around normal to orbit plane for short time periods and coarse retargeting for short time periods

- Effect of Time: Inverse linear consumption with manoeuvre duration.

The final selection of set of manoeuvres was based on a system trade-offs between available ΔV and required demonstration needs.

Non Experimental Phase

Between the exit from a controlled configuration mode and the acquisition of the required configuration at next observation mode, formation satellites must be manoeuvred with the main objective of minimising collision risk during perigee passage while saving as much propellant as possible. There are three main options:

- Free drift: directly leave the spacecraft to evolve naturally at the end of the experiment, without performing any loose formation acquisition phase.

- Direct transfer. Command a manoeuvre at exit from each experimental mode in order to acquire the desired relative position at entry of next experimental mode. Prior to arriving the new entry to apogee, a new manoeuvre would be commanded to acquire the correct relative velocity allowing the start of the science observation phase.

- Acquisition of a train formation. Command a manoeuvre at exit from each experimental mode in order to acquire a train formation (i.e., both satellites flying the same orbit one behind the other) before arriving the perigee. Afterwards, and before starting the next experimental mode, command satellites from the train formation to acquire the needed relative geometry (relative position and velocity);

Manoeuvre	Advantages	Disadvantages
Free Drift	· No consumption in loose formation acquisition	·Divergences of hundreds of meters · High cost of tight formation acquisition · Different behaviour depending on epoch · Collision avoidance is not assured
Direct transfer	· Simple and low cost · Collision avoidance through perigee is passively assured · Does not required complex dedicated tight formation acquisitions	· Collision avoidance not assured if braking manoeuvres fails
Acquisition of train formation	· Naturally stable formation · Robust passage by perigee · Behaviour independent of epoch · Collision free drift during several orbits	· Very high cost of acquisition of train formation · Geometry not directly related to mission return

Table 2 Comparison between strategies for non-experimental phase

Table 2 presents a comparison between them, based on the analyses performed. This leads to state that:

- Free drift transfer has an unpredictable behaviour and very expensive in terms of the need to acquire the formation after passage around the perigee

- Acquisition of a train formation for passive secure passage around the perigee very expensive in terms of loose and tight formation acquisition

- The baseline approach is to perform a direct transfer from an experimental formation to the following experimental formation by the application of a loose formation acquisition manoeuvre to perform a direct transfer and a tight formation acquisition manoeuvre stopping the formation evolution

The direct targeting is based on the use of transition matrix formulation for eccentric orbit. Without considering SRP, the transfer is very safe and the exact configuration for next experimental phase is reached. On the other hand, as seen in Figure 2-5, the effect of SRP can be very high, separating the spacecraft up to several hundred of meters.
To cope with the effect of the SRP, several options have been investigated and developed:

- To re-design the spacecraft to have similar SRP ballistic coefficients. It will not cost anything in terms of DV, but will have a deep impact at system level. This option is discarded
- To counteract continuously the effect of the SRP along the perigee passage. Simple, but costly and operationally risky
- Re-design the direct transfer manoeuvre considering implicitly in the manoeuvre the compensation of the effect of the SRP. This is the option selected, as it is operationally more simple and cheaper

The basic Direct Transfer (DT) manoeuvres implicitly compensating the SRP effect, shall be complemented by the application of one or more mid-course correction manoeuvres (MCM) during the perigee passage in order to compensate any error in the computation or execution of the baseline manoeuvres, and with the aim to target to the desired configuration for the next experiment.

This correction manoeuvre can be done any time after perigee passage, considering that there is relative navigation information available (e.g. RF measurements or differential GPS). This correction manoeuvre will lead the chaser to the appropriate location to start the experiment, compensating also for unexpected perturbations.

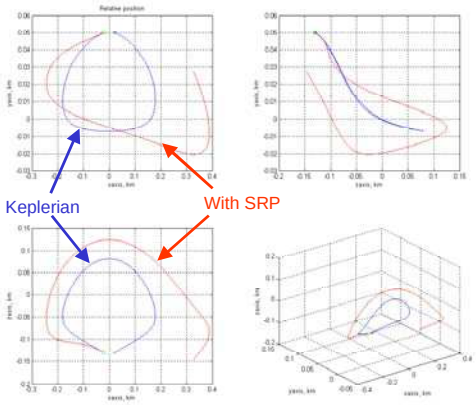

Figure 2-5 Example of the effect of SRP

In this sense, an important trade-off of the DT strategy is to select the number and location of the MCMs in order to basically minimize DV and dispersion at the end of the perigee (which in the end also translates into DV to build again the formation).

The implementation of 2 MCM or does not bring a significant benefit in terms of DV or final dispersion (see Figure 2-6), and on the other hand includes an operational complexity. Therefore, in order to reduce complexity while keeping a similar level of required DV, an strategy of 1 MCM at 0.5 h before the end of the perigee passage is retained as baseline. Figure 2-7 shows the overall cost of the DT strategy, and the cost of each manoeuvre of the strategy.

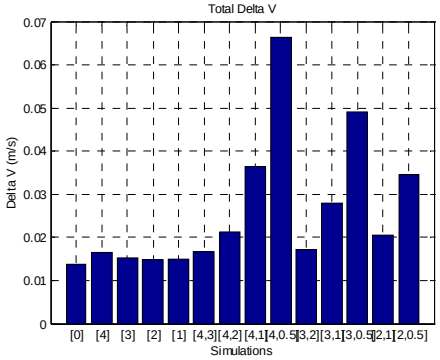

Figure 2-6 Comparison of DV of DT manoeuvres (top) for different combinations of MCMs

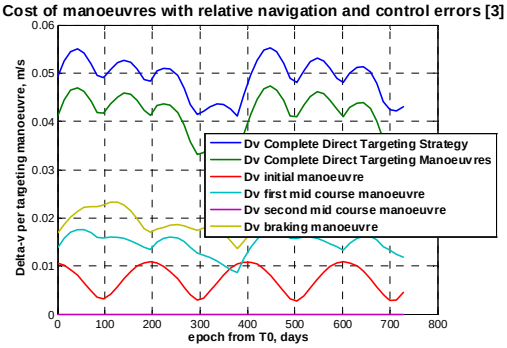

Figure 2-7 DV during the complete mission timeline for a DT with 1 MCM @ 0.5 h before the target and using Optical Metrology for the first manoeuvre.

3. GNC CONCEPT AND ALGORITHMS DESIGN

Based on the baseline mission scenario presented in previous section a specific GNC concept has been proposed and designed at algorithms level.

Following bullets presents a brief description of the different algorithms designed and implemented within a detailed and realistic Functional Engineering Simulator (FF-FES)

- **Guidance**: it will cope with its intrinsic two functionalities
  - Trajectory generation. This functionality is in charge of providing the position controller with the reference position to point the formation towards the Sun.
    Guidance takes, through the on-board ephemeris, the inertial direction to the Sun in terms of Right Ascension and Declination. Afterwards the on-board knowledge of the master vehicle orbital parameters allows to transcribing this into a reference position into LVLH frame.

  - Trajectory Control. It is in charge of generating the boost command to acquire the formation during different GNC modes such as Loose Formation, Tight Formation and Coarse Retargeting.
    The algorithm is based on the inversion of the Y-A transition matrix [1] with the inclusion of the particular solution taking into account the effect of the SRP.
    It is also in charge of providing the feed forward term during the nominal observation phase. This is done by imposing the required kinematics (see next bullet on trajectory generation) to the relative dynamics and computing the required acceleration.

- **Navigation**. a Navigation Performance Model for Formation Flying provides realistic accounts of estimates that would result from a consider Kalman filter formulation.
  A covariance analysis is performed to get realistic figure of the navigation accuracy in different operational conditions. Covariance is propagated and updated based on the assumption that RF metrology and optical sensors are available.
  Once the results from the covariance are available a random signal is generated. Its correlation time can be arbitrarily chosen so that its covariance is equal to that coming from the covariance propagation and update process. This signal is added to the real world measurements, thus simulating the output of a full navigation filter.

- **Control**. A closed loop controller has been designed and implemented for the Nominal Observation mode. Controller is based on the Non-Linear Dynamic Inversion (NDI) of the time varying plant of the relative motion into elliptical orbit.
  Desired dynamics is provided through a PID controller that has been designed in order to control the reference position modelling the plant with a second order dynamics.

Guidance Algorithm Design

- Trajectory Generation.
  Guidance algorithms for FF coronograph experiment and technology demonstration consist in applying the following process:

  - Generation of the required relative kinematics in the LVLH frame to conduct the desired relative motion, for example, inertial pointing or a resizing manoeuvre, starting from a given configuration. Eq. 1 shows an example of the desired LVLH relative kinematics based on the Sun declination (DEC) and Right Ascension (RAS) angles and the satellite ISD (D).
  - The relative kinematics is input in the relative motion equations for eccentric orbits (see Eq. 2), providing the required accelerations to fly the desired motion.

  - Relative position from Eq. 1 is used to feed the feedback controller (NDI), whereas the accelerations obtained from Eq. 2 are provided as a feed-forward to be added to the NDI command.

$$
\begin{aligned}
x &= D\cos(DEC)\cos(\nu - RAS);\\
y &= -D\cos(DEC)\sin(\nu - RAS);\\
z &= -D\sin(DEC);\\
\dot{x} &= -D\cos(DEC)\dot{\nu}\sin(\nu - RAS);\\
\dot{y} &= -D\cos(DEC)\dot{\nu}\cos(\nu - RAS);\\
\dot{z} &= 0.0;\\
\ddot{x} &= -D\cos(DEC)(\ddot{\nu}\sin(\nu - RAS) + (\dot{\nu}^2)\cos(\nu - RAS));\\
\ddot{y} &= D\cos(DEC)(\ddot{\nu}\cos(\nu - RAS) - (\dot{\nu}^2)\sin(\nu - RAS));\\
\ddot{z} &= 0.0;
\end{aligned}
\qquad \textbf{Eq. 1}
$$

$$
\begin{bmatrix} \ddot{x} \\ \ddot{y} \\ \ddot{z} \end{bmatrix} = \begin{bmatrix} -k\sqrt{\omega^3}x + 2\omega\dot{y} + \dot{\omega}y + \omega^2 x \\ -k\sqrt{\omega^3}y \\ 2k\sqrt{\omega^3}z - 2\omega\dot{x} - \dot{\omega}x + \omega^2 z \end{bmatrix} + \begin{bmatrix} a_x \\ a_y \\ a_z \end{bmatrix} \qquad \textbf{Eq. 2}
$$

With

$$
k = \frac{\mu}{\sqrt{h^3}}
$$

- Trajectory Control
  This component is in charge of providing the retargeting manoeuvre at the exit of the experimental phase and the MCM after the perigee passage.
  This manoeuvre is performed during the Loose Formation Acquisition mode aiming at entering in the next observation phase with the correct configuration. Trajectory control is computed using the transition matrix (for the relative dynamics) and a typical terminal point guidance algorithm.
  It consists in using the transition matrix of the dynamic model to derive the initial velocity as a function of the initial, final position and time of flight.
  Current state can be written as a function of the initial conditions using the transition matrix as reported in Eq. 3 where it has been split in four sub-matrices

$$
\begin{aligned}
\mathbf{r}(t) &= \Phi_{rr}(t)\mathbf{r}_0 + \Phi_{r\dot{r}}(t)\dot{\mathbf{r}}_0\\
\dot{\mathbf{r}}(t) &= \Phi_{\dot{r}r}(t)\mathbf{r}_0 + \Phi_{\dot{r}\dot{r}}(t)\dot{\mathbf{r}}_0
\end{aligned}
\qquad \textbf{Eq. 3}
$$

The velocity required to attain the final position can be derived properly inverting the Eq. 3

$$
\dot{\mathbf{r}}_0^+ = \Phi_{r\dot{r}}^{-1}\left(\mathbf{r}_1 - \Phi_{rr}\mathbf{r}_0\right) \qquad \textbf{Eq. 4}
$$

However for generating the retargeting command the dynamic model is upgraded using a semi-analytical formulation of the particular solution related with the solar radiation pressure (SRP) (see *Figure 3-1*). This particular solution represents the change in the final position due to the accumulated effect of the SRP during the time of flight (r_p).

This can be introduced in the scheme reported in Eq. 4 to derive the proper initial velocity to attain the prescribed final position taking into account the SRP

$$
\dot{\mathbf{r}}_0^+ = \Phi_{r\dot{r}}^{-1}\left(\mathbf{r}_1 - \mathbf{r}_p - \Phi_{rr}\mathbf{r}_0\right) \qquad \textbf{Eq. 5}
$$

This particular solution has been obtained by computing the relative dynamics response to a force that is constant in an inertial reference system, as SRP can be assumed during a limited time-of –flight (TOF < 1day).
This response is provided into a semi-analytical form. Some terms have to be evaluated through numerical quadrature being not available the primitive solution for that integral term.

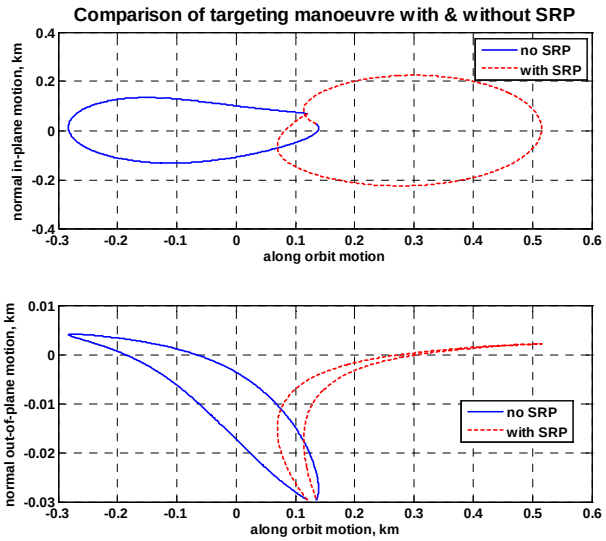

Figure 3-1 Comparison of targeting manoeuvre with and without SRP differential perturbation

This particular solution is based on the homogenous solutions provided by Yamanka-Ankersen [1] for the non-forced motion and implements the general approach proposed by Carter [2]

Navigation Algorithm Design

The Navigation Performance Model for Formation Flying provides realistic accounts of estimates that would result from a consider Kalman filter formulation. A Covariance analysis is performed to get realistic figure of the navigation accuracy in different operational conditions.

Over nominal trajectory, propagated by the algorithm itself, covariance is propagated and updated based on the assumption that RF metrology and optical sensors are available.

The Covariance Analysis module functional diagram is presented in *Figure 3-2*

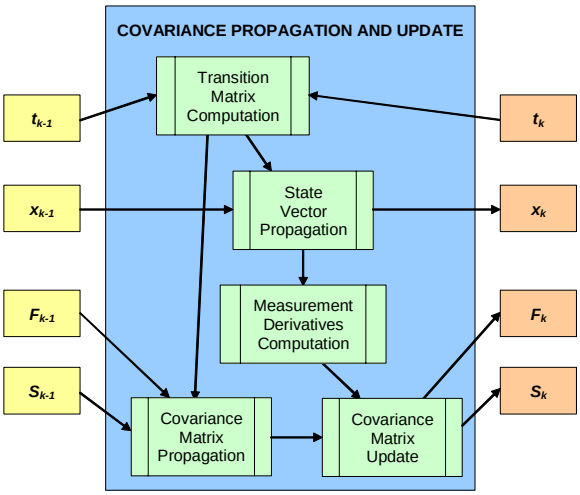

Figure 3-2 Covariance Analysis Functional Diagram

The Navigation Performance Model for Formation Flying assumes in its measurement derivatives computation step, as a baseline, that the following set of sensors is available:

- Optical Sensor will provide measurements of the projected direction of a number of beacons (reflecting cubes) with an accuracy of 5 μrad (1 σ)

- Ranging Sensor (possibly part of the LIDAR or RF) provides range measurements with an accuracy of 10 mm (1 σ)

The simulated error in the estimate is generated as an Exponentially Correlated Random Variable, with pre-set time-correlation:

$$x_0 = P_0 w_{noise}$$

$$x_{k+1} = e^{-\frac{dt}{\tau}} x_k + P_{k+1}\sqrt{1-e^{-2\frac{dt}{\tau}}}\, w_{noise} \qquad \textbf{Eq. 6}$$

Where:

- τ is the self-correlation time.
- dt is the step duration
- P_{k+1} is the updated covariance
- w_{noise} is band-limited Gaussian white noise, with a normal distribution of average 0 and covariance 1.

This generated signal is then added to the real world states so as to provide realistic simulated Kalman Filter estimates. *Figure 3-3* shows an example of how an ECRV can be modeled to the covariance. The standard deviation of position estimates during the first 200 seconds of a coronagraph experiment is obtained through the Covariance Analysis module. A number of shots generated using this data are plotted (in blue) together with the results from the covariance analysis (3σ , in black).

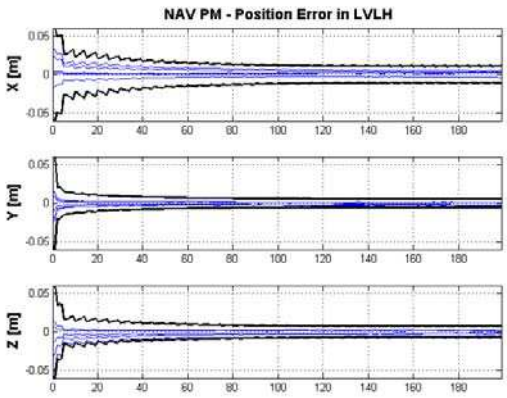

Figure 3-3 Example of navigation performance model Estimates -

Control Algorithm Design

A closed loop controller has been designed and implemented for the Nominal Observation mode. Controller is based on the Non-Linear Dynamic Inversion (NDI) of the time varying plant of the relative motion into elliptical orbit.
Desired dynamics is provided through a PID controller that has been designed in order to control the reference position modeling the plant with a second order dynamics.

NDI is a promising technology widely used in aircraft but that only recently has started being considered for space applications. It can be summarized as a three main step process, see *Figure 3-4*: definition of the controlled variable (CV), characterization of the desired dynamics and inversion of the dynamics. The objective is to achieve the desired response for the CV vector x to command vector xc, i.e. to drive the error vector xe to zero (xp in the figure refers to the feedback vector).

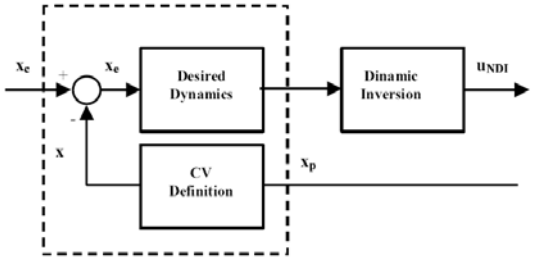

Figure 3-4 FF-NDI control architecture.

For the relative FF problem, the controlled variable definition consists of transforming the line-of-sight (LOS) and distance measurements into relative position and velocity vectors. Then, the desired dynamics is specified paralleling a standard ideal second-order representation. Finally, the dynamic inversion is performed and consists of two sub-steps: one the proper inversion of the dynamics and second, a control allocation scheme (typically, used when there are more control effectors than control variables).

In this article, we will focus only in the first two main steps: CV definition and desired dynamic achievement, since a main assumption is that the control distribution matrix is an identity. As the study was developed for a technological proof-of-concept this assumption suffices, but it is recognized that the subsequent step will be to implement realistic actuator models with magnitude limitations and invert the associated control effector distribution matrix and firing time limits (although there is already a simplex thrust allocation method implemented and used in the FES).

It is straightforward to derive the NDI control input $u_{NDI}=[f_x \quad f_y \quad f_z]^T$: from the short-hand version of the relative motion equations that can be written as reported in Eq. 7:

$$\begin{bmatrix} \ddot{x} \end{bmatrix} = \begin{bmatrix} \Gamma_1 & \Gamma_2 \\ I_3 & 0 \end{bmatrix} \begin{bmatrix} \tilde{x} \end{bmatrix} + \begin{bmatrix} I_3 \\ 0 \end{bmatrix} \begin{bmatrix} \tilde{f} \end{bmatrix} \qquad \textbf{Eq. 7}$$

The NDI controller action is given by

$$\begin{bmatrix} f_x \\ f_y \\ f_z \end{bmatrix}_{cmd} = -\begin{bmatrix} \Gamma_1 & \Gamma_2 \end{bmatrix} \tilde{x} + \begin{bmatrix} \ddot{x} \\ \ddot{y} \\ \ddot{z} \end{bmatrix}_{des} \qquad \textbf{Eq. 8}$$

Now, the question is how to obtain the desired, which represents the new desired commands. A classical control approach with 2nd order reference model will be followed.
First, note that although this is a second-order differentiation on the relative position vector this just means that we need a double integrator between the desired commands and the measured relative position vector. This is shown in Eq. 9

$$\begin{bmatrix} \ddot{x} \\ \ddot{y} \\ \ddot{z} \end{bmatrix}_{des} = PID_1 \left(\begin{bmatrix} \dot{x} \\ \dot{y} \\ \dot{z} \end{bmatrix}_{ref} - \begin{bmatrix} \dot{x} \\ \dot{y} \\ \dot{z} \end{bmatrix}_{meas} \right) \qquad \textbf{Eq. 9}$$

That can be written as:

$$\begin{bmatrix} \ddot{x} \\ \ddot{y} \\ \ddot{z} \end{bmatrix}_{des} = PID_1 \left(PID_2 \left(\begin{bmatrix} x \\ y \\ z \end{bmatrix}_{ref} - \begin{bmatrix} x \\ y \\ z \end{bmatrix}_{meas} \right) - \begin{bmatrix} \dot{x} \\ \dot{y} \\ \dot{z} \end{bmatrix}_{meas} \right) \qquad \textbf{Eq. 10}$$

Where PID1 and PID2 represent the standard Proportional-Integral-Derivative (PID) block found in most NDI controllers Now, note that rather than designing two sequential PID blocks, one for the relative position error and the other for the relative velocity error, it is possible to simplify the design process by comparison to the well-known ideal second-order model:

$$x = \frac{\omega^2}{s^2 + 2\xi\omega s + \omega^2} x_{ref} \qquad \textbf{Eq. 11}$$

Figure 3-5 shows the Closed Loop absolute errors for all axes. Due to the large initial closed-loop (CLP) reference command used in the CLP simulations, the time responses are divided in two sections: the left plots consider the first 2000 seconds of the simulation (to showcase the rise-time and overshoot characteristics for the CLP simulations) while the right plots show the rest of the simulation.

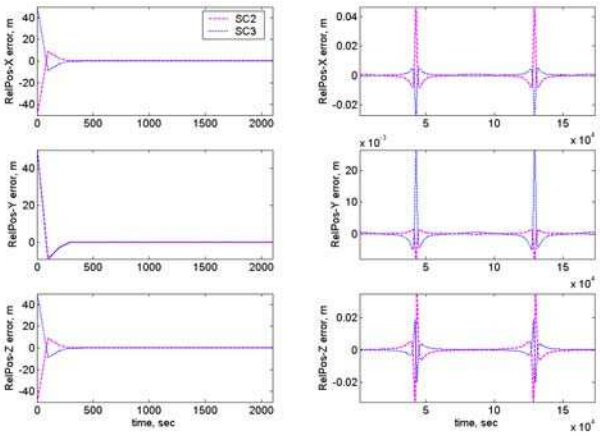

Figure 3-5 Closed Loop baseline: relative position error w.r.t. SC1 in LVLH frame

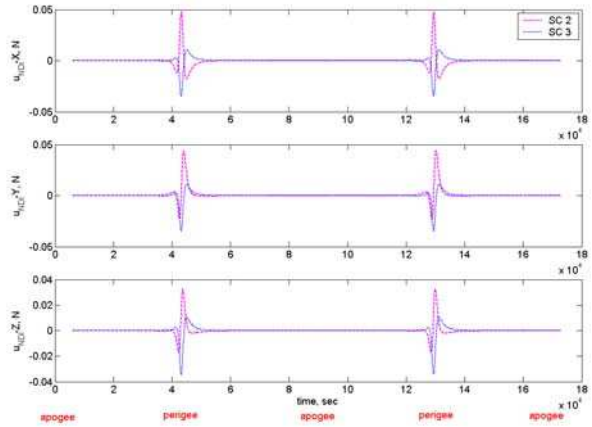

Figure 3-6 CLP baseline: commanded forces

It is observed that the worst errors achieved by the NDI FF-controller are respectively for each axis [0.04 0.02 0.025] meters and moreover, these are achieved at the perigee(s).

Figure 3-6 shows the demanded thrust (which can be used as an indicator for the fuel consumption). It is observed that a very small consumption with peaks around the perigee (of magnitude smaller than 0.05N) is demanded. For the rest of the orbit, it was appreciated that the thrust demanded was below 0.1 mN.

4. CONCLUSIONS

This paper has presented a complete formation flying mission analysis and GNC concept for a formation-flying mission in a highly eccentric orbit. Feasible solutions have been found and presented for the different challenges brought by flying on a non-circular orbit, specially due to the time varying nature of the relative motion.

5. ACKNOWLEDGMENTS

Part of the work presented in this paper was done in the frame of ESA/ESTEC study "GNC Algorithms for Rendezvous and Formation Flying in Non-Circular Orbits (GNCO)". Thanks are given to its ESA Technical Officer Rémi Drai, for his guidance and valuable comments.

Acknowledgments are also given to the Proba-3 project team

6. REFERENCES

[1] K. Yamanaka, F. Ankersen, "New State Transition Matrix for Relative Motion on an Arbitrary Elliptic Orbit", Journal of Guidance, Control, and Dynamics, Vol. 25, No 1, Jan-Feb 2002, pag 60–66

[2] Humi, M., "Fuel-Optimal Rendezvous in a General Central Force Field", Journal of Guidance, Control and Dynamics, Vol. 16, No.1, 1993